Chalmers Publication Library

CHALMERS

Copyright Notice

(Article begins on next page)

Comparison of polarization-switched QPSK and polarization-multiplexed QPSK at 30 Gbit/s

Martin Sjödin,[1] Pontus Johannisson,[1] Henk Wymeersch,[2]
Peter A. Andrekson,[1] and Magnus Karlsson[1]

[1]Photonics Laboratory, Department of Microtechnology and Nanoscience,
Chalmers University of Technology, SE-412 96, Göteborg, Sweden
[2]Communication Systems Group, Department of Signals and Systems,
Chalmers University of Technology, SE-412 96, Göteborg, Sweden
[*]martin.sjodin@chalmers.se

Abstract: We present the first experimental results for polarization-switched QPSK (PS-QPSK) and make a comparison with polarization-multiplexed QPSK. Our measurements confirm the predicted sensitivity advantage of PS-QPSK. We have also studied the single channel performance after transmission over 300 km and support the results with numerical simulations. It is shown that the two modulation formats have similar nonlinear tolerance and that optical dispersion compensation outperforms compensation with digital signal processing in the single channel case. Finally, we propose a novel transmitter for PS-QPSK based on an IQ modulator and two amplitude modulators driven in a push-pull configuration.

OCIS codes: (060.1660) Coherent communications; (060.0060) Fiber optics and optical communications.

References and links

[1] M. Karlsson and E. Agrell, “Which is the most power-efficient modulation format in optical links?,” *Optics Express*, vol. 17, no. 13, 10814-10819, 2009.
[2] P. Serena, A. Vannucci, and A. Bononi, “The performance of polarization switched-QPSK (PS-QPSK) in dispersion managed WDM transmissions,” in *European Conf. on Opt. Commun. (ECOC)*, p. Th.10.E.2, 2010.
[3] P. Poggiolini, G. Bosco, A. Carena, V. Curri, and F. Forghieri, “Performance evaluation of coherent WDM PS-QPSK (HEXA) accounting for non-linear fiber propagation effects,” *Optics Express*, vol. 18, no. 11, pp. 11360-11371, 2010.
[4] H. Sun, K.-T. Wu, and K. Roberts, “Real-time measurements of a 40 Gbit/s coherent system,” *Optics Express*, vol. 16, no. 2, pp. 873-879, 2008.
[5] L. E. Nelson, S. L. Woodward, S. Foo, X. Zhou, M. D. Feuer, D. Hanson, D. McGhan, H. Sun, M. Moyer, M. O Sullivan, and P. D. Magill, “Performance of a 46-Gbps dual-polarization QPSK transceiver with real-time coherent equalization over high PMD fiber,“ *J. Lightwave Technol*., vol. 27, no. 3, pp. 158-167, 2009.
[6] J.-X. Cai, Y. Kai, C. R. Davidson, D. G. Foursa, A. Lucero, O. Sinkin, W. Patterson, A. Pilipetskii, G. Mohs, and N. S. Bergano, “Transmission of 96x100G bandwidth-constrained PDM-RZ-QPSK channels with 300% spectral efficiency over 10610 km and 400% spectral efficiency over 4370 km,” to be published in *J. Lightwave Technol*., 2011.
[7] P. Johannisson, M. Sjödin, M. Karlsson, H. Wymeersch, E. Agrell, and P. A. Andrekson, “A modified constant modulus algorithm for polarization-switched QPSK,” submitted to *Optics Express*.
[8] A. J. Viterbi and A. M. Viterbi, “Nonlinear estimation of PSK-modulated carrier phase with application to burst digital transmission,” *IEEE Transactions on Information Theory*, vol. 29, no. 4, pp. 543-551, 1983.
[9] M. S. Alfiad, D. van den Borne, T. Wuth, M. Kuschnerov, B. Lankl, C. Weiske, E. de Man, A. Napoli, and H. de Waardt, ”111-Gb/s POLMUX-RZ-DQPSK transmission over 1140 km of SSMF with 10.7-Gb/s NRZ-OOK neighbours,” in *European Conf. on Opt. Commun. (ECOC)*, p. Mo.4.E.2, 2008.
[10] D. Wang and C. R. Menyuk, “Polarization evolution due to the Kerr nonlinearity and chromatic dispersion,” *J. Lightwave Technol*., vol. 17, no. 12, pp. 2520-2529, 1999.
[11] C. Behrens, R. I. Killey, S. J. Savory, M. Chen, and P. Bayvel, “Nonlinear distortion in transmission of higher order modulation formats,” *Photonics Technol. Lett*., vol. 22, no. 15, pp. 1111-1113, 2010.

1. Introduction

Polarization-switched quadrature phase-shift keying (PS-QPSK) is a modulation format that has received increasing attention recently. There are two major reasons for this: Firstly, it has been shown that PS-QPSK is the modulation format with the highest sensitivity. Compared to polarization-multiplexed QPSK (PM-QPSK), PS-QPSK has a sensitivity advantage of 0.97 dB at a BER of 10^{-3}, and an asymptotic advantage of 1.76 dB [1]. Secondly, simulation results have been presented showing that PS-QPSK has higher nonlinear tolerance in WDM transmission scenarios [2-3]. These features make PS-QPSK an interesting candidate for long-haul systems, for example transoceanic links. PS-QPSK transmits three bits per symbol, where two bits are encoded in the QPSK symbol and the third bit in the switching between the polarization states.

PM-QPSK has been extensively studied and results have been presented using online post-processing of the data at high symbol rates [4-5]. PM-QPSK has, together with binary PSK, the second highest sensitivity of all modulation formats in common use and with 4 bits per transmitted symbol it is more spectrally efficient than PS-QPSK. Recently, Cai *et al.* demonstrated transmission of 112 PM-QPSK channels at 112 Gbit/s over 9360 km with a spectral efficiency of 3.6 bit/(s Hz), by using aggressive pre-filtering and intersymbol interference mitigation after detection [6]. Such performance would be hard to match for most other modulation formats. However, the results that have been demonstrated so far show that PS-QPSK has the potential to perform equally well or better than PM-QPSK and that it deserves to be further investigated.

So far, analytical and numerical results have been presented. In this paper, we present the first experimental results and make a comparison with PM-QPSK both at the same bit rate (30 Gbit/s) and at the same symbol rate (10 Gbaud). We have studied the back-to-back sensitivity and found good agreement with theory. We have also studied the single channel performance after propagation in a link with 300 km of standard single-mode fiber (SSMF). Both optical dispersion compensation and compensation with digital signal processing (DSP) were investigated. We complemented our experiments with numerical simulations and found good agreement between experimental and numerical results.

In [1] it was shown that PS-QPSK can be obtained from the conventional PM-QPSK transmitter (two IQ modulators, one per polarization) by using two XOR gates to force the driving bits to have even parity. We here present an alternative transmitter based on a single IQ modulator (IQM) and two amplitude modulators driven in a push-pull fashion. We have also suggested and implemented a new algorithm for polarization demultiplexing of PS-QPSK [7].

2. Experiment

2.1 Transmitter

The PS-QPSK transmitter is shown in Fig. 1. The laser source was an external cavity laser (ECL) with 300 kHz linewidth and the wavelength was set to 1550 nm. 30 Gbit/s PS-QPSK was generated in two steps: First, an IQM driven by two 10 Gbit/s $2^{15}-1$ pseudo-random binary sequences (PRBS) generated Gray coded QPSK. In the second step, the QPSK signal was split into two branches, each containing a single-drive Mach-Zehnder modulator (MZM). The MZMs were driven in a push-pull configuration to switch the power on and off. As a result, only one polarization per symbol slot had non-zero power after recombination with a polarization beam-combiner (PBC). To synchronize the on-off switching between the two data streams, the lengths of the fibers between the amplitude modulators and the PBC were adjusted to be the same. It was also ensured that the total lengths of the two branches were approximately the same, to have high correlation between the phase noise in the x and the y polarization. The reason for using this transmitter is that we found this to be the most straightforward way to implement PS-QPSK in our lab. As shown in [1], PS-QPSK can also be generated with a PM-QPSK transmitter by using 8 of the 16 PM-QPSK symbols. Unless the amplitude modulators in the scheme proposed in this paper have low extinction ratio, the performance of the two different PS-QPSK transmitters should be similar. One advantage with the transmitter in Fig. 1 is that it requires only three data streams for PS-QPSK generation, while the other approach needs four.

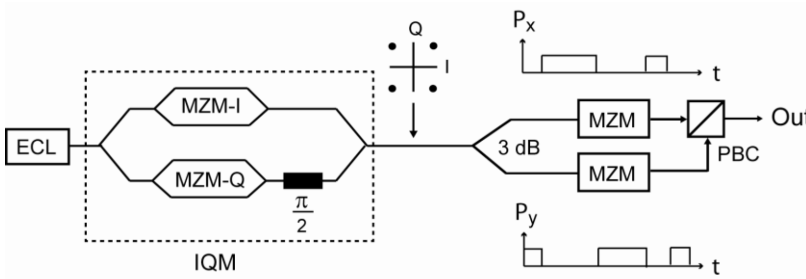

Fig. 1: The transmitter used to generate PS-QPSK. The amplitude modulators are driven in a push-pull configuration to switch between the two polarization states.

PM-QPSK was generated by the same transmitter but with the RF signals to the amplitude modulators turned off, and a piece of fiber with a length of 2 m (about 100 symbol slots at 10 Gbaud) was inserted in one path to decorrelate the data in the x- and the y-polarization. The output power after the transmitter was about −25 dBm for both PS-QPSK and PM-QPSK.

2.2 Receiver

The receiver is shown in Fig. 2. The same hardware was used for both modulation formats. An attenuator (Att) and an erbium-doped fiber amplifier (EDFA) with a noise figure of 5 dB were used to adjust the optical signal-to-noise ratio (OSNR) of the signal and a band-pass filter (BPF) with 0.3 nm bandwidth suppressed amplified spontaneous emission (ASE) noise outside the signal spectrum. Polarization diversity was obtained by splitting the signal with a polarization beam-splitter (PBS) and mixing the light in the x- and the y-polarization with the output from a local oscillator (LO) laser (an ECL with 500 kHz linewidth) in two optical 90° hybrids with integrated balanced detectors and electrical amplifiers. The combined 3 dB bandwidth of the detectors and the amplifiers was more than 25 GHz.

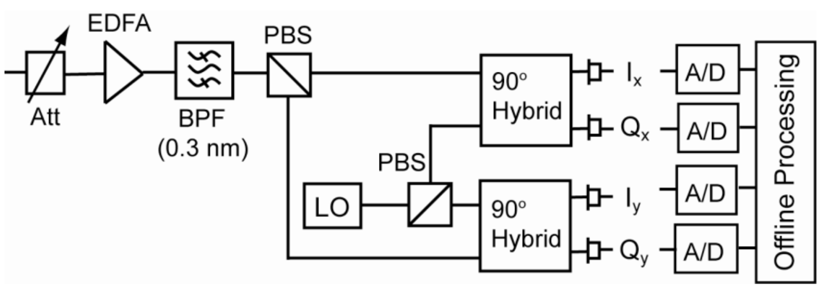

Fig. 2: The receiver used to detect PS-QPSK and PM-QPSK.

After photodetection the signals were sampled synchronously at 50 Gsample/s by a real-time sampling oscilloscope with 16 GHz analog bandwidth. Offline DSP was then used to perform the following four tasks:

(i): Low-pass filtering of the signals with a 5^{th} order Bessel filter with the bandwidth equal to a factor of 0.75 times the symbol rate (7.50 GHz and 5.63 GHz for 30 Gbit/s PS-QPSK and PM-QPSK, respectively) to ensure a fair comparison between the modulation formats. We also tried other bandwidths, but did not see any performance improvements.

(ii): Polarization demultiplexing and equalization with an adaptive filter with a length of three symbols. In this step the signal was also down-sampled to one sample per symbol. The equalization improved the performance with about 1 dB in the numerical simulations for both modulation formats.

(iii): Compensation for the intermediate frequency between the signal laser and the LO laser. The frequency peak resulting from the beating between the lasers was obtained from the spectra of the complex photocurrents raised to the fourth power. The intermediate frequency was then removed by a linear phase shift on the data streams.

(iv): Phase noise estimation with the Viterbi and Viterbi algorithm [8].

In the polarization demultiplexing, the conventional CMA was first tried for both modulation formats. Unfortunately, it turned out that it cannot be used for PS-QPSK since there is not a unique demultiplexing matrix that achieves the constant modulus property for this modulation format. We therefore replaced CMA with a new algorithm, which is described in detail in [7]. It uses the cost function

$$J = \mathrm{E}\left[\frac{1}{2}\left(\left|i_x\right|^2 + \left|i_y\right|^2 - P\right)^2 + \left|i_x\right|^2\left|i_y\right|^2\right], \tag{1}$$

where E is the expectation operator, i_x and i_y are the complex photocurrents from the two polarization states and P is the total average power. Eq. (1) is minimized when a QPSK symbol is transmitted in one of the polarization states while the power in the other state is zero.

In the phase estimation process for PS-QPSK, a decision was first made to determine if the QPSK symbol had been transmitted in the x- or the y-polarization by comparing the amplitude of the samples from the two polarization states. The sample with the highest amplitude was selected for phase estimation. For PM-QPSK, phase estimation was performed separately for the data in the two polarizations.

After removal of the laser phase noise, bit-errors were counted. For PS-QPSK, one bit was decoded by deciding in which polarization the QPSK symbol had been launched. The optimal way to do this is to select the polarization that yields

$$\max\left(\left|i_{\mathrm{x,r}}\right| + \left|i_{\mathrm{x,i}}\right|,\ \left|i_{\mathrm{y,r}}\right| + \left|i_{\mathrm{y,i}}\right| \right), \tag{2}$$

where r and i denote the real and imaginary parts of the two photocurrents i_x and i_y. However, selecting the photocurrent with the largest amplitude only leads to a very small penalty compared to when (2) is used. A detailed derivation of (2) is beyond the scope of this paper. The remaining two bits were decoded by making a decision on the QPSK symbol. With the transmitter in Fig. 1, the bit-to-symbol mapping is the same as the one suggested in [1], which means that the six most (and equally) likely symbol errors will have 1.5 bits incorrect on average.

2.3 Link

The link used in the transmission experiment is shown in Fig. 3. It consisted of four spans with 75 km of standard single-mode fiber (SSMF) preceded by EDFAs. We tried compensation for chromatic dispersion (CD) with both dispersion compensating fiber (DCF) and with DSP. When optical dispersion compensation was used, an additional section with an EDFA followed by DCF was inserted after each SSMF span. As in [9], the power launched into the DCF was set to be 5 dB lower than the SSMF launch power. The signal power was monitored with an optical spectrum analyzer to ensure that the ASE noise power from the EDFAs was not included in the launch power values. When dispersion compensation with DSP was used, it was performed in Fourier domain as the first step after the coherent detection.

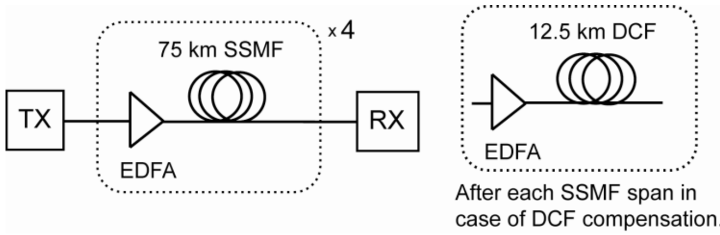

Fig. 3: The link used in the transmission experiment.

For each SSMF launch power, the OSNR at the receiver required to obtain a BER of 10^{-3} was determined. The OSNR was varied by using the attenuator and the EDFA in Fig. 2.

3. Numerical simulations

To support the experimental results, we have carried out numerical simulations of both 10 Gbaud PS-QPSK and PM-QPSK at 7.5 and 10 Gbaud. As a model for light propagation in an optical fiber, we used the Manakov model together with attenuation [10]

$$i\frac{\partial \mathbf{E}}{\partial z} = \frac{\beta_2}{2}\frac{\partial^2 \mathbf{E}}{\partial t^2} - \gamma\left(\mathbf{E}^{\mathrm{H}}\mathbf{E}\right)\mathbf{E} - i\frac{\alpha}{2}\mathbf{E}, \qquad (3)$$

where $\mathbf{E}=(E_x,E_y)^{\mathrm{T}}$ is the complex envelope of the two polarization components, β_2 is the group-velocity dispersion parameter, γ is the Kerr nonlinearity parameter, α is the attenuation and $^{\mathrm{H}}$ denotes Hermitian conjugation. The equation describes propagation in a fiber with rapidly and randomly varying birefringence, which is the case for most sufficiently long transmission fibers. Polarization-mode dispersion was neglected.

Three 2^{15} sequences of random data in the form of square pulses were used to generate PS-QPSK. Two sequences encoded the QPSK symbol and the third sequence encoded the switching between the two polarization states. To generate PM-QPSK, four sequences were used. To emulate the experiment, all optical signals were band-limited to 10 GHz by a raised-cosine filter before they entered the transmission line, and the transmitter output power was set to −25 dBm.

The simulated link was similar to the one shown in Fig. 3 with four spans of 75 km SSMF preceded by EDFAs. The performance was simulated for both optical dispersion compensation and compensation with DSP after detection. In the case of DCF compensation a section with an EDFA followed by DCF was inserted after each SSMF span. The parameter values for the different components in the simulations are shown in Table 1.

Table 1: Fiber and Link Parameters

	SSMF	DCF
α [dB/km]	0.2	0.4
D [ps/(nm km)]	17	−105
γ [1/(W km)]	1.2	5.3
Inline EDFA noise figure [dB]	5	

After transmission, additional ASE was added and the OSNR required to achieve a BER of 10^{-3} was determined. At least 250 bit errors were counted. Before the receiver, a 0.3 nm first-order Gaussian band-pass filter removed power outside the signal spectrum and after detection the signals were low-pass filtered by a 5$^{\text{th}}$ order Bessel filter with the same bandwidths as in the experiment. Laser phase noise was not included in the simulations, but the same equalizers as in the experiment were implemented.

4. Experimental and numerical results

The figures in this section should be read according to Table 2.

Table 2: Figure legend

Modulation format	Measured	Simulated	CD comp. (Figs. 5 and 6 only)
10 Gbaud PS-QPSK	◆	◇	DCF ——
7.5 Gbaud PM-QPSK	✱	✳	
10 Gbaud PM-QPSK	▼	▽	DSP - - - -

The measured back-to-back BER as a function of OSNR for both PS-QPSK and PM-QPSK are shown in Fig. 4. PS-QPSK requires 7.9 dB OSNR to obtain a BER of 10^{-3}, compared to 8.6 dB for PM-QPSK at the same bit-rate. The difference of 0.7 dB in favor of PS-QPSK agrees quite well with the value predicted in [1] (0.97 dB). At the same symbol rate the measured difference between the two modulation formats is 2.2 dB, which is equal to the theoretical prediction. The performance given by the analytical results from [1] for the three cases is included in Fig. 4. The measured PS-QPSK sensitivity is 1.3 dB lower than the theoretical prediction at the given BER of 10^{-3}. For PM-QPSK, the differences are 1.3 dB and 1.0 dB at 10 Gbaud and 7.5 Gbaud, respectively. This explains to a large extent why we measure 0.7 dB difference instead of 0.97 dB when we compare PS-QPSK and PM-QPSK at the same bit-rate. The 0.3 dB penalty is most likely due to bandwidth limitations in the transmitter, since the components in the receiver have bandwidths significantly larger than the symbol rates used in the experiment. It can also be observed in Fig. 4 that the difference between the analytical and the measured BER curves is getting slightly larger when the OSNR increases. The reason for this is likely intersymbol interference (ISI).

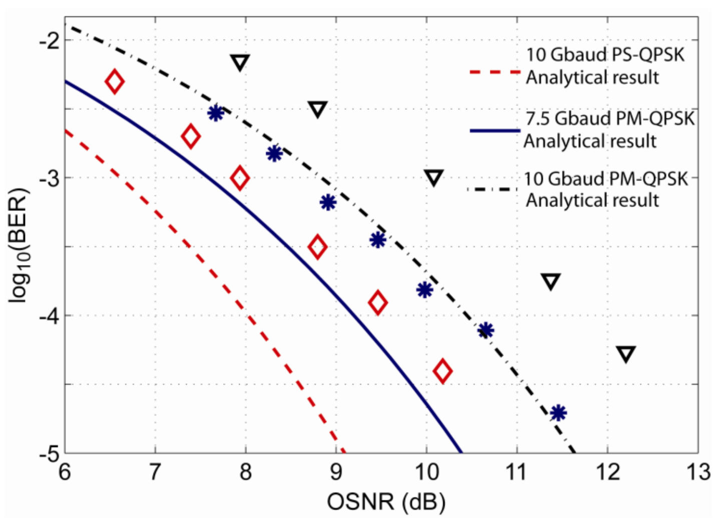

Fig. 4: The measured back-to-back BER measurements for 10 Gbaud PS-QPSK and PM-QPSK at both 10 and 7.5 Gbaud. The theoretical OSNR requirements are also shown for each case.

The measured and simulated OSNR required to obtain a BER of 10^{-3} as a function of the launch power into the SSMF spans is shown in Figs. 5a and 5b, respectively. The three signals behave similarly in both the measurements and the simulations, and it is apparent that higher launch power can be used when the dispersion is compensated with DCF instead of DSP. This is in good agreement with [11], in which the authors conclude that single channel NPSK formats perform better in links with optical dispersion compensation. The reason for this is decreased pulse overlap compared to links in which the dispersion is compensated after detection. It is worth mentioning that in WDM transmission the behavior can be significantly different [3]. The simulated sensitivity in the linear regime at a BER of 10^{-3} was about 0.3 dB worse than the analytical sensitivity. The reason for this is ISI in the transmitter and non-matched receiver filters.

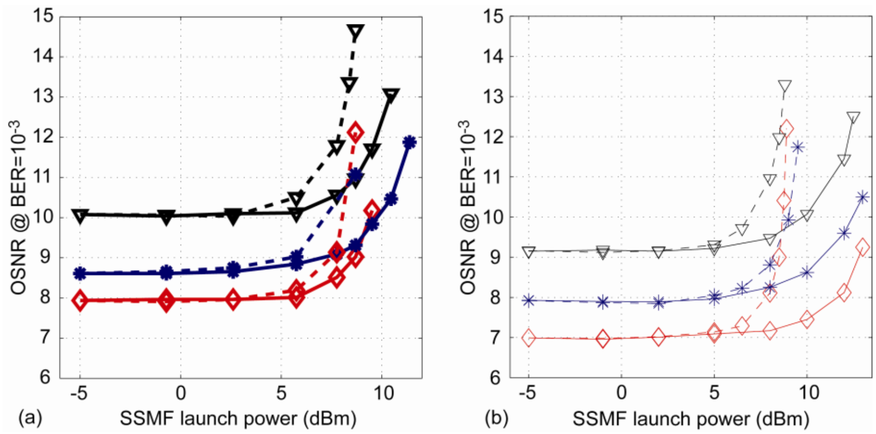

Fig. 5: The OSNR requirements @ BER=10^{-3} for 10 Gbaud PS-QPSK and PM-QPSK at 7.5 and 10 Gbaud as a function of the launch power into the SSMF spans in the link. (a) Measured results. (b) Simulated results.

Fig. 6a-c show the measured results together with the corresponding simulation results for the three signals. For PS-QPSK and PM-QPSK at 10 Gbaud, the required OSNR in the linear regime is about 1 dB lower in the simulations compared to the measurements. For PM-QPSK at 7.5 Gbaud, the difference is about 0.7 dB. These results seem reasonable taking into account the non-ideality of the components in the experiment. For example, the driving signals to the modulators have both distortion and noise.

We investigated the launch power at an OSNR penalty of 1 dB compared to the linear regime for both the experimental and the numerical results for the three cases. The agreement between the experimental results and the simulations is very good for DSP compensation of dispersion. The difference in launch power at 1 dB penalty between the experimental results and the simulation results is less than 0.5 dB for all three cases.

For DCF compensation, the launch power at 1 dB penalty is 3.0, 1.5 and 1.3 dB lower in the measurements compared to the simulations, for PS-QPSK, 7.5 Gbaud PM-QPSK and 10 Gbaud PM-QPSK, respectively. We believe the explanation for the larger difference between measurements and simulations is the increased number of system parameters when DCF compensation is used, such as the input power to the DCF modules and the additional EDFAs and splice losses, making it more difficult to model everything accurately.

When comparing with the WDM simulation results in [2] and [3], it is apparent that the benefit of PS-QPSK over PM-QPSK is much smaller in the single channel case. The explanation for this is that PS-QPSK has higher tolerance than PM-QPSK to cross-channel effects such as cross-polarization modulation [2], which is beneficial in WDM transmission.

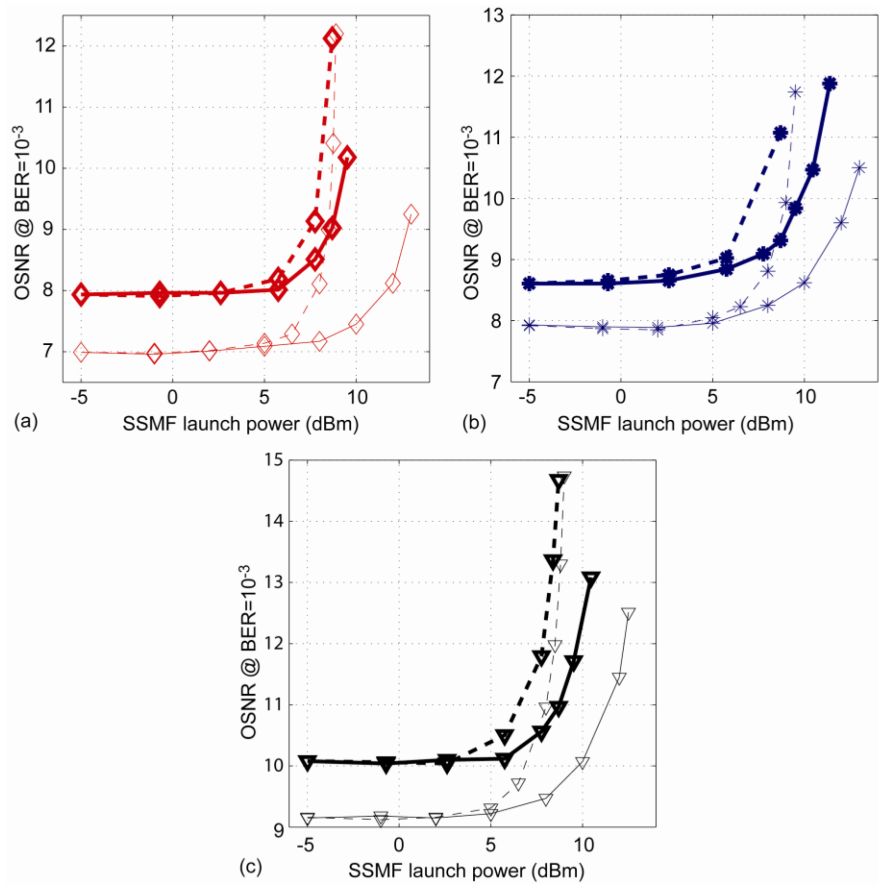

Fig. 6: Simulated and measured results for the OSNR requirements @ BER=10^{-3} as a function of the launch power into the SSMF spans in the link. (a) 10 Gbaud PS-QPSK. (b) 7.5 Gbaud PM-QPSK. (c) 10 Gbaud PM-QPSK.

5. Conclusion

We have performed the first experimental investigation of polarization-switched QPSK and verified that it achieves higher sensitivity than QPSK with polarization-multiplexing. When comparing the two modulation formats at the same bit rate, the OSNR required to achieve a BER of 10^{-3} was 0.7 dB lower for PS-QPSK. The reason for not reaching the theoretical difference of 0.97 dB is bandwidth limitations in the transmitter that penalized PS-QPSK more than PM-QPSK due to its higher symbol rate.

The transmission experiment and the numerical simulations both showed that in the single channel case, PS-QPSK has similar nonlinear tolerance as PM-QPSK, both at the same symbol rate and at the same bit rate. Optical dispersion compensation permitted higher launch power into the SSMF spans than DSP based compensation. This agrees well with previously published simulation results.

Acknowledgments

We acknowledge the financial support from the Swedish research council, the Knut and Alice Wallenberg foundation, the Vinnova IKT program, and the EU EURO-FOS project. We also acknowledge discussions with Erik Agrell about the optimum choice of polarization state in which a PS-QPSK symbol has been transmitted. This work was performed within the Fiber Optic Communications Research Center (FORCE) at Chalmers.